

Karbala International Journal of Modern Science

Manuscript 3353


Synthesis of Dyes Sulfamidazole: Characterization, Evaluation, Molecular Docking and Global Descriptors by Density Functional Theory (DFT).

Athra G. Sager

Jawad Kadhim Abaies

Zeena R. Katoof

Follow this and additional works at: <https://kijoms.uokerbala.edu.iq/home>

 Part of the [Biology Commons](#), [Chemistry Commons](#), [Computer Sciences Commons](#), and the [Physics Commons](#)

Synthesis of Dyes Sulfamidazole: Characterization, Evaluation, Molecular Docking and Global Descriptors by Density Functional Theory (DFT).

Abstract

In the present work, novel azo compounds of sulfamidazole were created via the reaction of diazonium salt of sulfamidazole with several aromatic molecules including (resorcinol, 2-nitro phenol, 3-nitro phenol, and 4-nitro phenol) (Z1–Z4). The new compounds (Z1-Z4) were identified using FTIR, ¹HNMR techniques, in addition to melting point measurements. The biological activity of compounds (Z1-Z4) was studied against four kinds of bacteria including *E. coli*, *Klebsiella pneumonia*, *Salmonella*, and *Staphylococcus aureus*. The findings showed that all compounds (Z1-Z4) were active against the examined bacteria. Theoretical studies of the antibacterial ability of the prepared compound against DNA gyrase enzyme using MOE.2015 were performed. Also, studying their inhibition ability against tested bacteria in vacuum media was carried out theoretically. This was achieved using the DFT [6-311/B3LYP⁺G (2d, 2p)] method.

Keywords

Density Functional Theory; Dyes; HOMO-LUMO; Molecular Docking; Sulfamidazole

Creative Commons License



This work is licensed under a [Creative Commons Attribution-Noncommercial-No Derivative Works 4.0 License](https://creativecommons.org/licenses/by-nc-nd/4.0/).

RESEARCH PAPER

Synthesis of Dyes Sulfamidazole: Characterization, Evaluation, Molecular Docking and Global Descriptors by Density Functional Theory (DFT)

Athra G. Sager*, Jawad K. Abaies, Zeena R. Katoof

Department of Chemistry, College of Science, University of Waist, Kut, Iraq

Abstract

In the present work, novel azo compounds of sulfamidazole were created via the reaction of diazonium salt of sulfamidazole with several aromatic molecules including (resorcinol, 2-nitro phenol, 3-nitro phenol, and 4-nitro phenol) (Z1–Z4). The new compounds (Z1–Z4) were identified using FTIR, ¹HNMR techniques, in addition to melting point measurements. The biological activity of compounds (Z1–Z4) was studied against four kinds of bacteria including *Escherichia coli*, *Klebsiella pneumonia*, *Salmonella*, and *Staphylococcus aureus*. The findings showed that all compounds (Z1–Z4) were active against the examined bacteria. Theoretical studies of the antibacterial ability of the prepared compound against DNA gyrase enzyme using MOE.2015 were performed. Also, studying their inhibition ability against tested bacteria in vacuum media was carried out theoretically. This was achieved using the DFT [6-311/ B3LYP⁺G (2d, 2p)] method.

Keywords: Density functional theory, Dyes, HOMO–LUMO, Molecular docking, Sulfamidazole

1. Introduction

Azo compounds are a class of organic compounds that gained a lot of attention by scientific community. These compounds are distinguished by their brightly-colored [1]. So, they have been widely utilized in dyes and paint synthesis [2–4]. Due to the exceptional thermal and optical features of azo compounds, they have many applications in different fields. For instance, they use as toner, ink-jet printing, and visual recording medium [5]. Also, they have been labelled as anti-diabetic, anti-neoplastic and antibacterial agents [6], in addition to their use as anticancer drug [7]. Restraining DNA, RNA and tumorigenesis are other uses of azo compounds [8,9]. One of the sulfa drugs with a sulfonamide antimicrobial activity is 4-amino-N-(4-methylpyrimidin-2-yl) benzene sulfonamide (AMBPS). This drug is a powerful inhibitor for bacteria that resist tetracycline, and considered a potent agent for treating infectious

diseases including pneumonia, tuberculosis and leprosy [10]. In addition to its use in treatment of wastewater, AMBPS used as a high-value agent in biological researches. The AMBPS binding with sulfamerazine resulting in obstructing RNA synthesis, which lead to inhibition of growth of bacteria. Also, it is thought that congestive heart failure is affected by AMBPS- sulfadiazine hydrogen bonds [11]. As vital bacterial enzymes, DNA gyrase and topoisomerase IV considered a necessary objects in development of new antibacterial drugs [12,13]. In addition to invention and improvement of new antibiotics, rising the efficiency of the antibiotic that in use represents the ultimate strategy of researchers for facing antibiotic resistance [14]. Due to the significant applications in industry and biology like antibacterial [15,16], antitumor [17], enzyme inhibitors [18], and chelating material [19], amino phosphonates have been drawn much interest of the scientists. The important applications of these materials make

Received 7 February 2024; revised 17 April 2024; accepted 19 April 2024.
Available online 31 May 2024

* Corresponding author.

E-mail addresses: asker@uowasit.edu.iq (A.G. Sager), jabaies@uowasit.edu.iq (J.K. Abaies), zeenarazaq22@gmail.com (Z.R. Katoof).

<https://doi.org/10.33640/2405-609X.3353>

2405-609X/© 2024 University of Kerbala. This is an open access article under the CC-BY-NC-ND license (<http://creativecommons.org/licenses/by-nc-nd/4.0/>).

them favorable drugs for extra development. In the field of drug synthesis and optimization, amino phosphonates are regarded as auspicious substances as they are phosphorus correspondents of α -amino acids (naturally formed) [20]. This work aims to synthesize new azo sulfamidazole (sulf) derivatives and test their antibacterial activity towards DNA gyrase enzyme via MOE 2015 program. Global reactivity descriptors of the compounds are calculated to understand their stability, structures, and reactivity via parameters of quantum mechanics utilizing the DFT [6-311/ B3LYP⁺G (2d, 2p)] method.

2. Experimental

2.1. Chemicals and apparatus

Most solid chemicals and solvents were acquired from Sigma–Aldrich and used directly without additional purification. Sulfamidazole was purchased from the state company for drug industries and medical appliances (SDI) in Samarra, Iraq.

2.2. Instruments

Infrared spectra were recorded using a Shimadzu FT-IR 8400. ¹H NMR spectra were carried out using a Bruker machine at 400 MHz. All theoretical calculations were achieved using a computer Intel (core i7)/hp, RAM (64), Gaussian-View6.0, and the program Gaussian 09W.

2.3. Procedure for synthesis of diazonium salt (S1)

A concentrated hydrochloric acid (2.5 ml, 11.6N) was added to (10 mmol) of Sulfamidazole with 10 ml distilled water, and then cooled in an ice bath for 10 min [21]. A solution of sodium nitrate (NaNO₂) (0.70g, 1 mmol in 10 ml) water was added to sulfamidazole solution and stirred for 25 min in an ice bath at (0-5) °C. The precipitate was kept for synthesizing of dyes.

2.4. General procedure for synthesis of phenolic dyes (Z1-Z4)

A series of phenol derivatives compounds including resorcinol, 2-nitro phenol, 3-nitro phenol and 4-nitro phenol (10 mmol) were mixed with (50 ml, 10%) sodium hydroxide solution. The mixture was then cooled to below 5 °C. The produced sodium phenolate solutions were added carefully (drop by drop) to diazonium chloride solution (mentioned before) with continuous stirring. The mixture was left stirring at a temperature below

5 °C for half an hour. The precipitated material was separated and collected. Then, it was firstly rinsed by cold methanol before it was rinsed by cold water [22]. The obtained product was left to dry at room temperature for 24 h to form crystalline dyes with red, brown, orange and yellow color. FTIR spectra of Sulfamidazole dyes and their physical properties are shown in Table 1 and Table 2.

2.5. Study of antibacterial activity

The azo compounds (Z1-Z4) were tested against four strains of bacteria (*Escherichia coli*, *Klebsiella pneumonia*, *Salmonella*, and *Staphylococcus aureus*). The tests used the diffusion plate's technique in disc-agar. The experiments were carried out at the research laboratory, College of Science, Wasit University. Four bacteria strains were grown and incubated for 1 day at 37 °C. Furthermore, a concentration (100 µg/ml) of the synthesized compounds in DMSO was prepared [23]. To demonstrate the compound activity towards the examined bacteria strains after one day, inhibition zone was utilized to incubate the sample. The formed solutions activities of created compounds were compared with the activity of standard drug (Sulfamidazole). In equal amount of the produced solutions (20 ml), filter paper (Whatman no.3 with size of 6 mm) was soaked. Discs with both naturally formed and synthesized products were employed to wrap Muller Hinton agar.

2.6. Molecular docking study

The computerized method that is commonly employed for the binding orientation prediction of simple drug molecule, and subsequently prediction of the molecule activity and affinity towards a protein, is referred as insilico molecular docking. Aiming to recognize the interactions between the created molecules (Z1-Z4) with the enzyme DNA-gyrase (MOE-2014.0901) software was utilized to carry out molecular docking study. For every compound, an upper limit of 30 conformers was considered in the docking method. The visualization of the ligand - receptor binding interactions was conducted.

Table 1. Physical properties of compounds (Z1-Z4).

Code	Physical properties			
	M.p °C	solvent	color	Yield%
Z1	202–204	Ethanol	Red	76
Z2	213–215	Ethanol	brown	63
Z3	223–225	DMSO	orange	80
Z4	218–220	Ethanol	yellow	73

Table 2. FT-IR spectral data of azo compounds (Z1-Z4).

Comp	Major FTIR Absorption (cm^{-1})				
	$\nu(\text{O-H})$	$\nu(\text{C-H})$ Aliph	$\nu(\text{C-H})$ Arom	$\nu(\text{N=N})$	$\nu(\text{C=C})$ Arom
Z1	3410	2733–2991	3069–3148	1472	1591
Z2	3237	2734–2994	3064–3124	1453	1555
Z3	3247	2887–2947	3166–3051	1454	1532
Z4	33448	2748–2909	3017–3138	1449	1570

ChemDraw Professional 15.0 was utilized to draw all the created compounds (Z1-Z4). Energy minimization was run on Chem3D Ultra 15.0 with the MMFF94 force field. Protein Data Bank (BDP) was the source of the crystal structure of the enzyme DNA gyrase (PDB ID: 1KZN). The resolution that was greater than 2.30\AA and comprising the gene code of the same bacterial was the principle for the protein selection. Eliminating the clorobiocin in the sequence editor technique was applied to prepare the enzyme. A molecule of H_2O was introduced in the active sites to guarantee the generation of hydrogen bond between the ligands and the target. This attributed to significant role of H_2O molecule located in the active site of the targeted enzyme.

Prior to the adding of hydrogen atoms, the missing and broken bonds because X-ray diffraction were corrected by the protein structure. Docking and scoring calculations were performed utilizing the Molecular Operating Environment (MOE-2014.0901). As it is stated, the RMSD values perfect score is closer to 2\AA and the energy of score should be $= -7\text{ kcal/mol}$ or less value. In order to verify the docking results, these values were employed as a standard value [24,25].

2.7. Study of absorption, distribution, metabolism, excretion and toxicity (ADMET)

In the field of drug designing, because of the unfortunate drug properties and various undesired effects, several drugs did not succeed in clinical trials and subsequent development processes. In this work, all optimized compounds were investigated by the online web tool Swiss ADME. While, insilico, toxicity evaluation were conducted utilizing an online server ProTox-II, which exhibited anticipated oral toxicity, cytotoxicity, mutagenicity, carcinogenicity, hepatotoxicity, and values of immune toxicity of molecules (Z1-Z4).

2.8. Calculations models

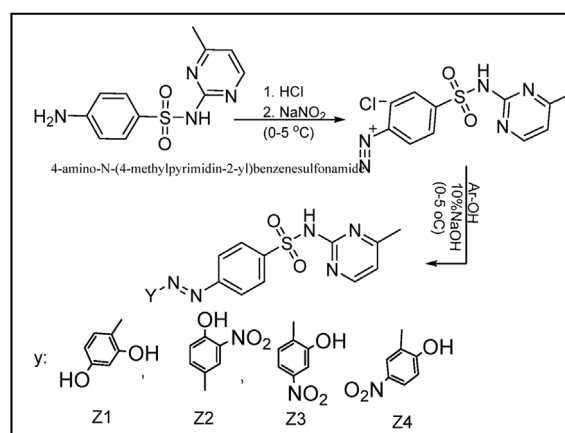
In the theoretical study, the compounds (Z1-Z4) were studied using (Gaussian 09W and Gauss View 6.0) program. The quantum chemical calculations

were carried out using density functional theory (DFT) with function (B3LYP), 6-311G⁺(d, p) basis range was utilized. This function provides precise electronic properties and geometries for organic compounds and gives similar results [26]. The calculations have been carried out under vacuum.

3. Results and discussion

3.1. Characterization

In this study, all dyes (Z1-Z4) were synthesized by coupling reaction between diazonium salt (electrophile) with sodium phenolate via an electrophilic aromatic substitution reaction. Scheme 1 explains the reaction steps synthesis of dyes (Z1-Z4). FTIR spectra of sulfamidazoles (Z1-Z4) showed absorption bands at ($3410, 3237, 3247$ and 3448) cm^{-1} attributed to OH -phenol groups, respectively ($3069-3148, 3064-3124, 3166-3051$ and $3017-3138$) cm^{-1} assigned to C-H aromatic in Z1-Z4, respectively. ($2733-2991, 2734-2994, 2887-2947,$ and $2748-2909$) cm^{-1} belong to aliphatic C-H, and ($1591, 1555, 1532$ & 1570) cm^{-1} due to C=C. FT-IR measurements data of azo-molecules (Z1-Z4) are shown in Table 2. FT-IR spectra of the prepared azo compounds (Z1-Z4) showed the disappearance of absorption band of NH_2 in sulfamidazole. Moreover, FT-IR spectra exhibited the presence of (N=N) bands at ($1472, 1453, 1454,$ and 1449) cm^{-1} , which is a proof for



Scheme 1. Preparation route of the compounds Z1-Z4.

formation the targeted compounds [27]. ^1H NMR spectra of compounds (Z1–Z4) are shown in Table 3 and Figs. 1–2.

3.2. The activity of azo compounds against bacterial

Antibacterial activity of Sulfamidazole derivatives (Z1–Z4) against four types of bacteria, including *E. coli*, *K. pneumonia*, *Salmonella*, and *S. aureus*, were also determined using Sulfamidazole as a reference, and DMSO as solvent. The compounds Z1, Z3 and Z4 were found to be highly active against all types of bacteria, whereas, the compound Z2 was found to be medium active against *S. aureus* and *Salmonella*. But this compound (Z2) showed a weak activity against *K. pneumonia*, and *E. coli*. Table 4 exhibits

antibacterial activity data. Fig. 3 shows the inhibitory effects around each disc.

3.3. Study theoretical to antibacterial activity

The compounds (Z1–Z4) were subjected to docking into the binding site of the DNA-gyrase (PDB code 1KZN) to evaluate their capabilities in inhibition the disease. The acquired results are listed in Table 5. The molecular docking score of molecules (Z1–Z4) fluctuated from (–5.7038 to –6.2705) kcal/mol, and the RMSD extended from 2.0374 to 2.3957 Å (see Fig. 4). Moreover, the optimal ligand binds with a particular receptor occurs when RMSD value about 2 Å and the energy equal to –7 kcal/mol [26,28]. These two values were dependent as standards to verify the molecular docking data. Table 5 displays

Table 3. ^1H NMR spectral data of compounds (Z1–Z4).

Cod.	Name	^1H NMR (400 MHz, DMSO- d_6 , δ / ppm)
Z1	(Z)-4-((2,4-dihydroxyphenyl)diazanyl)-N-(4-methylpyrimidin-2-yl) benzenesulfonamide	2.82 (s, 3H, methyl), 6.5–8.31(9H, Ar–H), 10.1(s, H, phenol). 11.9(s,H,HNSO $_2$)
Z2	(Z)-4-((3-hydroxy-4-nitrophenyl)diazanyl)-N-(4-methylpyrimidin -2-yl) benzenesulfonamide	2.42 (s, 3H, methyl), 6.7–8.4(9H,Ar–H), 12.4(s, H, phenol). 11.34(s,H,HNSO $_2$)
Z3	(Z)-4-((3-hydroxy-5-nitrophenyl)diazanyl)-N-(4-methylpyrimidin -2-yl) benzenesulfonamide	2.51 (s,3H,methyl), 6.90–8.779(9H,Ar–H), 9.98(s, H, phenol).
Z4	(Z)-4-((2-hydroxy-5-nitrophenyl)diazanyl)-N-(4-methylpyrimidin -2-yl) benzenesulfonamide	2.505 (s,3H,methyl), 6.86–8.24(9H,ArH), 11.7(s,H,HNSO $_2$), 12,51(s,H,phenol).

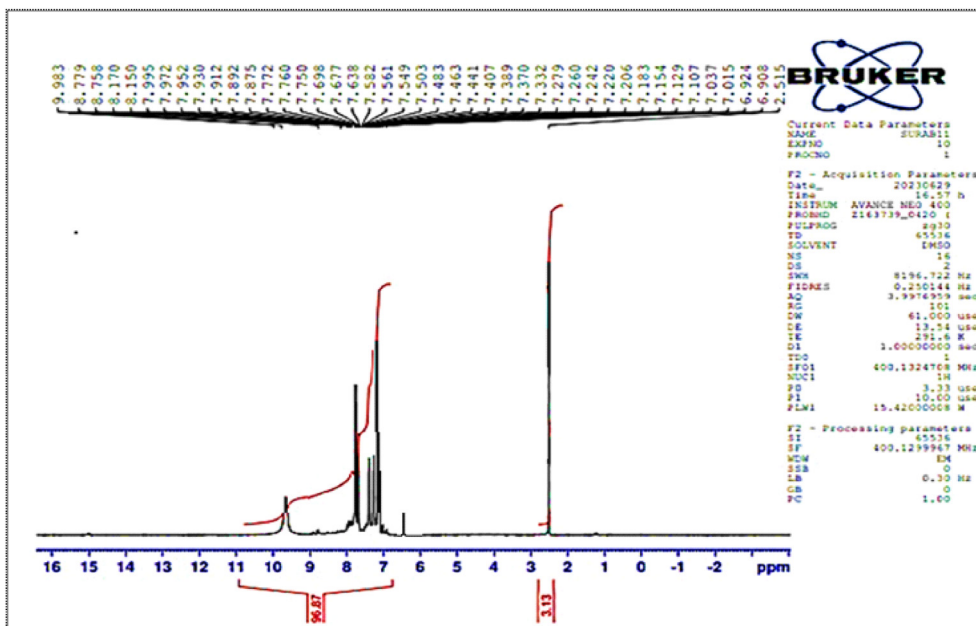


Fig. 1. ^1H NMR spectral data of compound Z3.

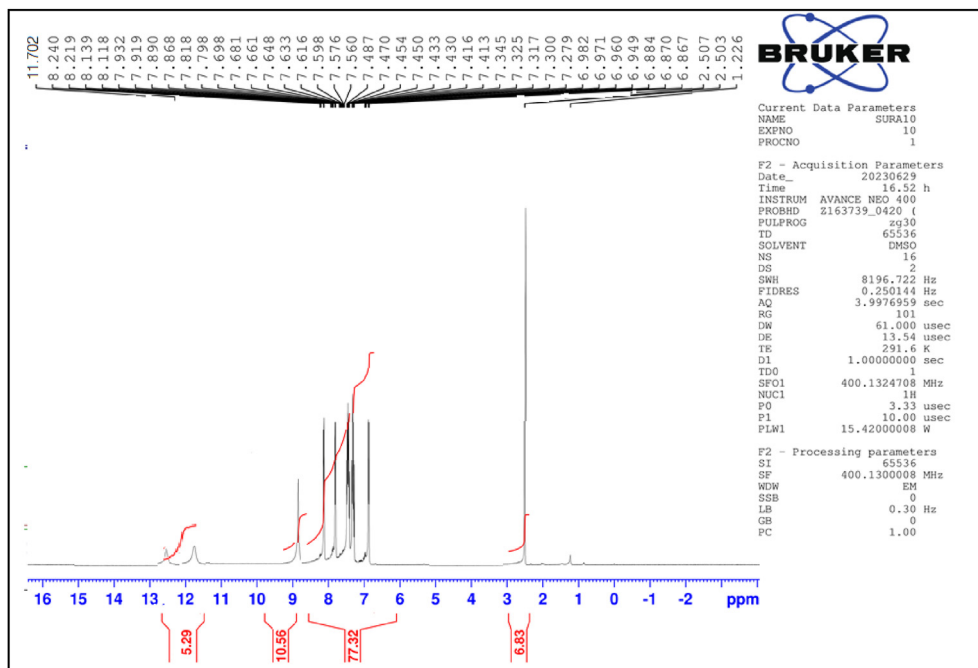


Fig. 2. ^1H NMR spectral data of compound Z4.

Table 4. Activity of compounds (Z1-Z4) against bacteria.

code	<i>E. coli</i>	<i>Staphylococcus aureus</i>	<i>Klebsiella pneumoniae</i> ,	<i>Salmonella</i>
Z1	10	14	15	16
Z2	8	14	8	12
Z3	12	14	10	16
Z4	12	15	14	17
Sulfamidazole (sulfa)	20	16	—	—
DMSO	—	—	—	—

the obtained results of the examined compounds, which indicated good molecular docking scores. The compounds Z2 and Z4 have the highest docking score -6.2705 and -6.2108 kcal/mol, respectively.

3.4. Study ADME properties

To design novel compounds for drug industry and development, the physicochemical properties play

very important function and must be taken into account. Molecular weight (MW), the heavy atoms number, hydrogen bond acceptors (HBA), hydrogen bond donors (HBD), rotatable bonds, molar refractivity, and topological polar surface areas (TPSA) are the molecule parameters that used to assess a drug-likeness profile. The calculation of compounds Z1-Z4 parameters were performed and listed in Tables 5–8. The drug-likeness profiles were computed according to Lipinski's ($MW \leq 500$; $HBA \leq 10$ and $HBD \leq 5$), Ghose's ($160 \leq MWt \leq 480$; $40 \leq MR \leq 130$ and $20 \leq \text{atoms} \leq 70$), Veber's.

(rotatable bonds ≤ 10 and $TPSA \leq 140$), Egan (TPSA ≤ 131.6) and Muegge ($200 \leq MW \leq 600$; aromatic rings number ≤ 7 ; various rotatable bonds ≤ 15 ; $HBA \leq 10$ and $HBD \leq 5$) [29,30]. The rule-based score describes the molecules into four possible score categories i.e. 11%, 17%, 55%, and 85%. The satisfactory possibility score is 55%, which

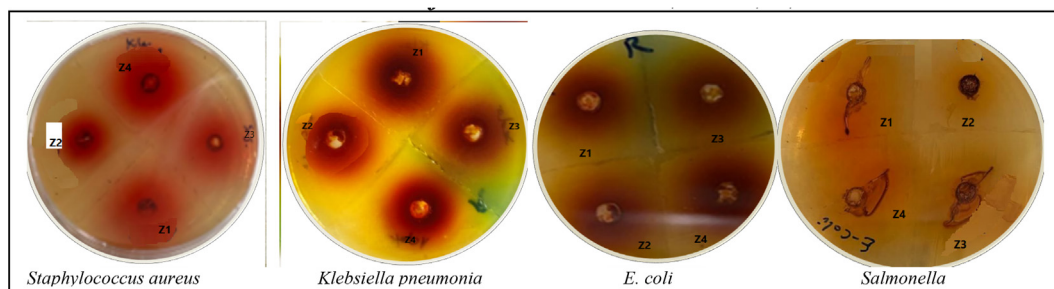


Fig. 3. The inhibitory effects around each disc.

Table 5. Molecular docking and RMSD data of the tested molecules (Z1-Z4).

No.	Score (kcal/mol)	RMSD (Å)	Bonds between Atoms of Compounds and Residues of Active Site of					
			Compd. atoms	Receptor atoms	Receptor Residues	Interaction	d(Å)	E (kcal/mol)
Z1	-5.7038	2.3957	O	OD1	ASP73	H-D	2.25	-2.3
Z2	-6.2705	2.0374	6-ring	N	VAL120(A)	Pi-H	4.40	-0.1
Z3	-5.9650	2.0843	O	OE1	GLU50(A)	H-D	2.32	-0.6
Z4	-6.2108	2.1239	—	—	—	—	—	—
Ligand (Clorobiocin)	-5.8172	2.0414	5-ring	CD	ILE78	Pi-H	3.97	-0.6
sulfa	-5.9634	2.1354	6-ring	CD	Pro79	Pi-H	4.24	-0.7

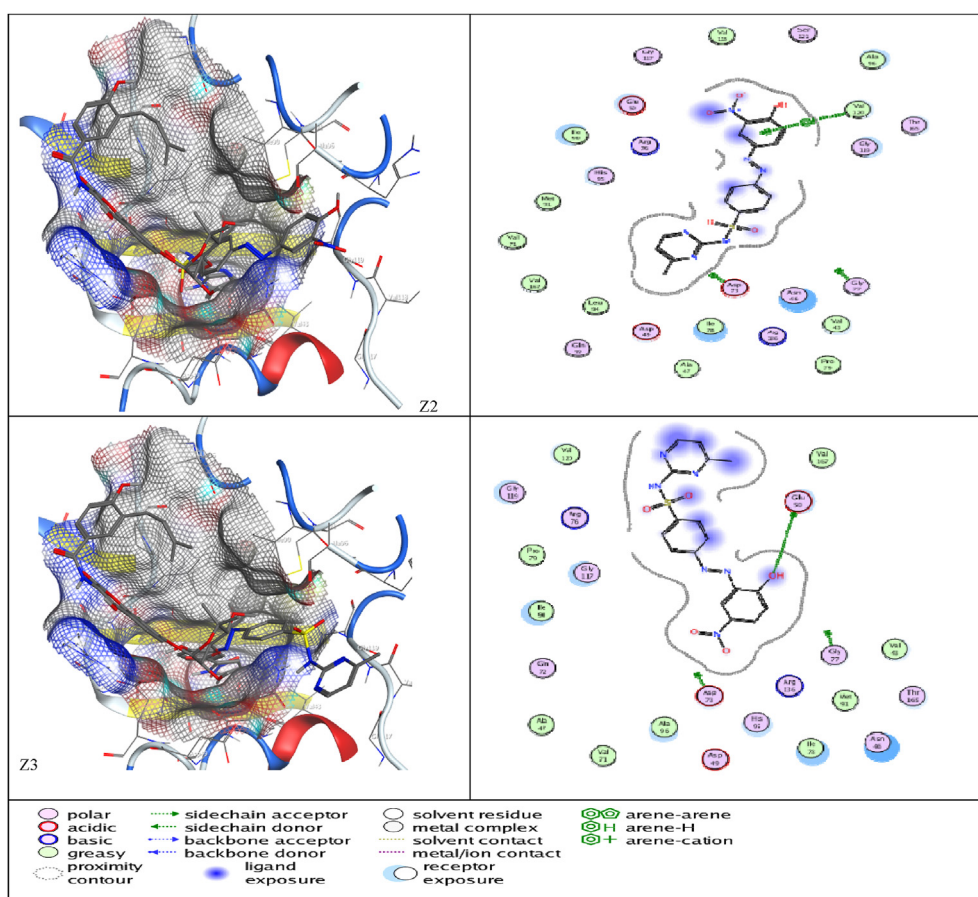


Fig. 4. Binding affinity of compounds Z2 –Z3 with DNA-gyrase.

designates that it fulfilled the rule of five. The tested molecules Z1-Z4 have appeared with a score of 85%, which indicates that they agreed all the five rules with adequate bioavailability. Furthermore, the created compounds availability was evaluated for quantifying the molecular structure complexity. The findings disclosed that the score varied from 2.37 to 3.32. This demonstrates that the compounds do not have a complex synthetic route as shown in Table 5. The expected lipophilicity mean data was evaluated and computed aiming for the determination of the compounds solubility medium (whether it is

aqueous or not) taking into consideration log Po/w assent value. Accordingly, the most negative value of log Po/w lead to the highest solubility of the compound. The findings disclosed that the molecules Z1-Z4 are soluble in non-aqueous media. Furthermore, the nature of solubility is designated by assent log S value. In this regards, very weak solubility: log S value less than -10, moderate: log S less than -6, good: log S less than -4, very good: log S less than -2, and high: log S less than O(18). The produced compounds were proposed to display a little GI absorption and deficiency of blood-brain

Table 6. Physicochemical properties of synthesized compounds Z1-Z4.

NO.	Formula	MWt. (g/mol)	Heavy atoms	HBA	HBD	Rotatable Bonds	Fraction Csp ³	Molar Refractivity	TPSA (Å ²)
Z1	C ₁₇ H ₁₅ N ₅ O ₄ S	385.40	27	8	3	5	0.06	98.78	145.51
Z2	C ₁₇ H ₁₄ N ₉ O ₅ S	414.40	18	9	2	6	0.06	105.57	171.10
Z3	C ₁₇ H ₁₄ N ₉ O ₅ S	414.40	18	9	2	6	0.06	105.57	171.10
Z4	C ₁₇ H ₁₄ N ₉ O ₅ S	414.40	18	9	2	6	0.06	105.57	171.10
Sulf.	C ₁₁ H ₁₂ N ₄ O ₂ S	264.30	12	4	2	3	0.09	68.52	106.35

Table 7. Drug likeness, bioactivity and synthetic accessibility score.

Code.	Lipinski	Ghose	Weber	Egan	Muegg	bioactivity Score	Synthetic accessibility
Z ₁	Yes; 0 violation	Yes	No, 1Violation. TPSA>140	No, 1Violation. TPSA>131.6	Yes	0.55	3.10
Z ₂	Yes; 1violation: Nor O > 10	Yes	No, 1Violation. TPSA>140	No, 1Violation. TPSA>131.6	No, 1Violation. TPSA>150	0.55	3.21
Z ₃	Yes; 1violation Nor O > 10	Yes	No, 1Violation. TPSA>140	No, 1Violation. TPSA>131.6	No; 1violation: TPSA .150	0.55	3.32
Z ₄	Yes; 1violation Nor O > 10	Yes	No, 1Violation. TPSA>140	No, 1Violation. TPSA>131.6	No; 1violation: TPSA .150	0.55	3.28

Table 8. Predicted absorption and distribution parameters of compounds Z1-Z4.

Compd.	lipophilicity		Water Solubility			pharmacokinetics			
	Consensus Log Po/w	Log Po/w (SILICOS-IT)	Consensus Log S (ESOL)	Solubility Class	(cm/s)LogS (SILICOS-IT)	Solubility Class	GI	BBB	Log Kp (cm/s)
T1	2.06	1.71	-3.58	soluble	-5.93	Moderately soluble	Low	No	-7.31
Z2	1.81	0.05	-4.12	moderately soluble	-5.86	Moderately soluble	Low	No	-6.97
Z3	1.65	0.05	-3.78	soluble	-5.86	Moderately soluble	Low	No	-7.36
Z4	1.68	0.05	-3.78	Soluble	-5.86	Moderately soluble	low	No	-7.36
sulf	0.72	0.21	-1.86	Very soluble	-4.18	Moderately soluble	High	No	-7.81

permeate. Resulting in severe brain toxicity and there is no possibility for bloodstream. It was designated that when log Kp with a greater negative value, skin permeates will be lesser. Accordingly, Z1-Z4 compounds exhibited the lowest skin permeate. This attributed to the high values of negative log Kp of these molecules as shown in Table 8. In addition to the bioavailability of drugs, metabolism has a significant role in drug–drug interactions. Also, metabolism parameters are necessary to recognize whether a molecule has an inhibition activity against certain proteins or not. The evaluation results of metabolism parameters of prepared compounds, Z1-Z4, exhibited that all these compounds were non-substrates of permeability glycoprotein (P-gp). This protein (P-gp protein) is

essential for evaluating active efflux via biological membranes and cytochrome P450 (CYP) enzymes. Moreover, it is noticed that Z1-Z4 compounds were non-substrates of CYP2D6 inhibitor, while Z2 and Z3 compounds were found to be substrates of CYP3A4. Nevertheless, all molecules were determined as substrates of CYP2C9 inhibitor, while all molecules were non-substrates of CYP₂C₁₉ inhibitor as shown in Table 9.

3.5. Toxicity prediction results

The toxicity of compounds (Z1-Z4) were calculated using ProTox-II online software [31] (see Table 10). Organ toxicity results suggested that compounds (Z2-Z3) were predicted to be hepatotoxicity, while

Table 9. Predicted metabolism parameters of the compounds (Z1-Z4).

Compd.	p-gp substrate	CYP1A2 inhibitor	CYP2C19 inhibitor	CYP2C9 inhibitor	CYP2D6 inhibitor	CYP3A4 inhibitor
Z1	No	Yes	No	Yes	No	No
Z2	No	Yes	No	Yes	No	Yes
Z3	No	No	No	Yes	No	Yes
Z4	No	Yes	No	Yes	No	Yes
Sulf.	No	No	No	No	No	No

Table 10. *Insilco toxicity evaluation of the compounds (Z1-Z4).*

Code	Organ Toxicity	Toxicity - endpoints				Predicted LD50 (mg/kg)
	Hepatotoxicity	Carcinogenicity	Immunotoxicity	Mutagenicity	Cytotoxicity	
Z1	–	+	–	–	–	25000
Z2	+*	+	–	–	–	25000
Z3	+	+	–	–	–	25000
Z4	+	+	–	–	–	25000
Sulf	–**	+	–	–	–	25000

**inactive; *active.

toxicological endpoint data indicated that all compounds with no mutagenicity and no cytotoxicity. All molecules were predicted to be carcinogenic. The compounds (Z1-Z4) were non- Mutagenic. The toxicity classes for all compounds were 6. LD50 describes the amount at which half of examined subjects die after being exposed to the tested molecule. Based on the globally harmonized classification system of chemical substances labelling (GHS), classes of toxicity are described. Class I: deadly if consumed ($LD50 \leq 5$); Class II: deadly if consumed ($5 < LD50 \leq 50$); Class III: toxic if consumed ($50 < LD50 \leq 300$); Class IV: destructive if.

Consumed ($300 < LD50 \leq 2000$); Class V: can destructive if consumed ($2000 < LD50 \leq 5000$), and Class VI: non-toxic ($LD50 > 5000$) [32].

3.6. Global reactivity descriptors

By the B3LYP scheme at 6-311 G⁺(d, p) level, the geometric parameters optimization of Z1-Z4 azo dyes. The calculations were done without

corrections of solvent. The calculations converged to a minimum accurate energy that was reinforced by the lack of imaginary frequencies. Consistent with the pattern of atom numbering, the final optimized compound structures were achieved an illustrated in Tables 11 and 12. Accordingly, calculations of several structural parameters including bond distances and bond angles were performed. Through the molecular orbital borders, the energy dependence inverse of the orbital energy difference stability, $\Delta E = E_{LUMO} - E_{HOMO}$, participates in the authoritarian contribution. Electrons donation mostly done by molecules that have high values of EHOMO. Moreover, energy of HOMO (E HOMO) can express the capability electron transfer. Tendency of molecule to accept electron is evaluated by energy of LUMO (E LUMO). Molecular activity characterizing also governed by vital factor, which is the energy gap (ΔE) between the orbital borders, where its efficiency improves when the energy gap is slight [33]. Global reactivity indices have important properties that authorize us to know the

Table 11. *Selected molecular structure parameters of compounds Z1 and Z2.*

Compound Z1				Compound Z2			
Bond length (Å)		Bond angles (Å)		Bond angles (Å)		Length Bond (Å)	
N19N11	1.24	N19N11C10	107.52	N19N11C10	107.25	N19N11	1.24
C23O27	1.35	C24C23O27	119.97	C24N41O42	118.39	N41O42	1.19
O26C21	1.35	O26C21C20	119.98	C23O26H39	108.01	C23O26	1.35
N12C1	1.34	N12C1N16	126.04	N2S3O4	109.48	N2S3	1.69
O4S3	1.45	O4S3C5	109.42	C15N16C1	115.59	C15N16	1.43

Table 12. *Selected molecular structure parameters of compounds Z3 and Z4.*

Compound Z3				Compound Z4			
Bond angles (Å°)		Bond length (Å)		Bond angles (Å°)		length (Å) Bond	
N16N24C25	107.5	1.24904	N16N24	C42N23O24	119.48	N23O24	1.31
C36N41O42	60.3	1.24807	N41C36	C40N20N12	107.48	N20N12	1.249
C34O15H1	108.007	1.35430	C34O15	C1O21H38	119.99	C1O21	1.355
N39S29O18	109.423	1.44983	S29O18	N3S4O18	109.47	S4O18	1.449
C22N23C27	115.58	1.3453	N23C27	N3C39N17	117.01	N3C39	1.352
C27N19C20	115.62	1.34197	C27N19	N3N13C39	116.95	N13C39	1.342
C34C28N16	119.98	1.25963	C28N16	C16N17C39	115.64	N17C39	1.342
N39C27N23	116.99	1.26571	C27N39	C41C42N22	120.03	C42N22	1.248

Table 13. DFT calculations of the inhibitors under vacuum medium at the equilibrium geometries as calculated using DFT method.

code	IE(eV)	EA (eV)	ω (eV)	S	η (eV)
Z1	4.026832	2.763651	9.125899	1.583304	0.631591
Z2	4.923195	3.545451	13.01367	1.451649	0.688872
Z3	5.219806	3.914446	15.97923	1.532145	0.65268
Z4	7.154035	4.156089	10.66721	0.667123	1.498973

code	HOMO (eV)	LOMO (eV)	ΔE (eV)	μ (Debye)	χ (eV)
Z1	-4.02683	-2.76365	1.26318	2.923977	3.395241
Z2	-4.92231	-3.54545	1.37774	7.148079	4.234323
Z3	-5.21980	-3.91444	1.30536	5.419016	4.567126
Z4	-7.15403	-4.15608	2.99795	8.843941	5.655062

chemical reactivity and kinetic stability of compounds as ($\mu = -\chi$), the absolute electronegativity (χ) is identified as ($\chi = (IP + EA)/2$), global hardness and global softness (S) is stated as ($\eta = (E_{LUMO} -$

$E_{HOMO})/2$) and ($S = 1/2\eta$), the electrophilicity (ω) can be calculated using the electronic chemical potential and the chemical hardness ($\omega = \mu/2\eta$). The improved density distributions of LUMO and HOMO for vacuum-phase compounds are displayed in Table 13 and Fig. 5. Regarding the electron density, red denotes a high value, whereas green denotes a low value. The surface electrons that were trapped represented by the green region [34–36]. Therefore, consideration of these two regions distribution is too important. The electronic density around the receptor was very high due to the atom's nonbonding electrons were in the N=N arrangement. Although all molecules have a high electronic density and belongs to the double bond and aromatic molecule area, the receptor site is mostly aromatic.

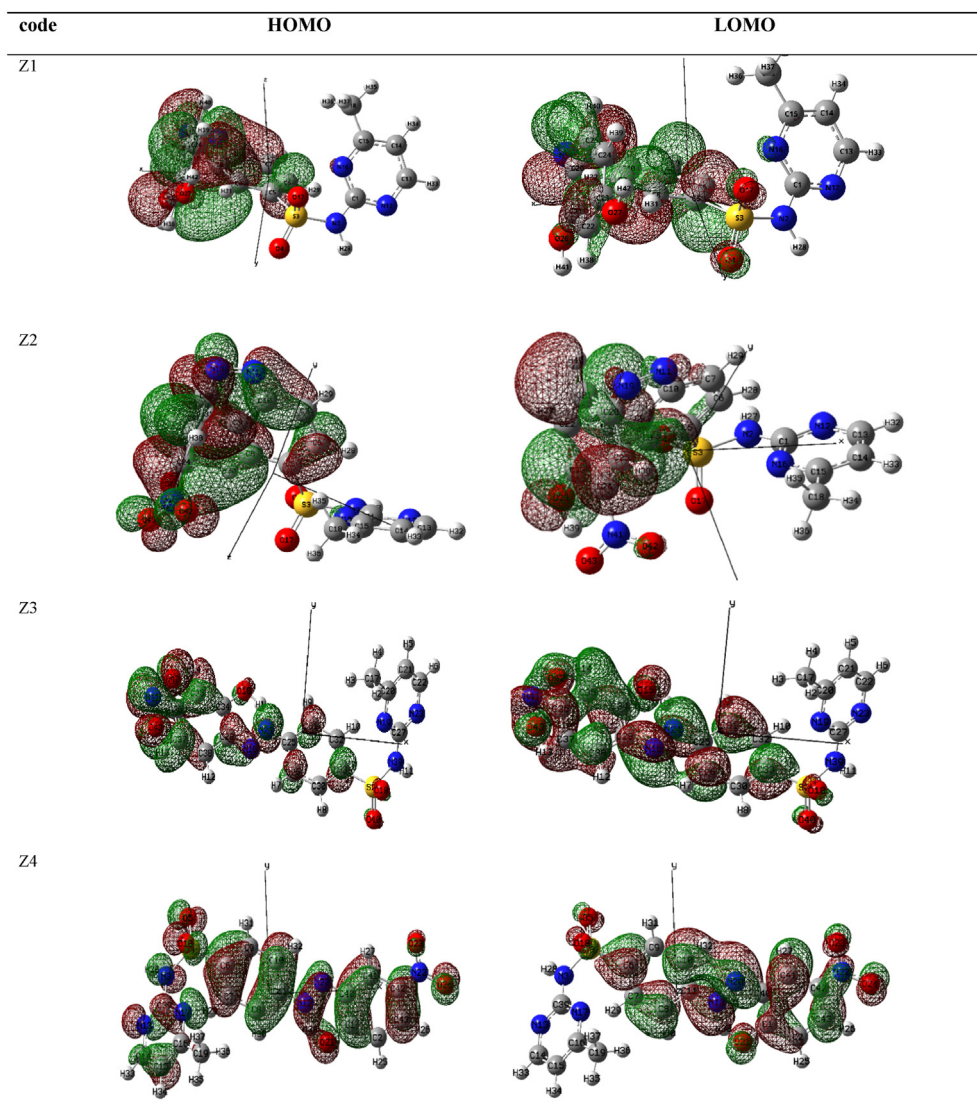


Fig. 5. The orbitals energy levels (HOMO–LUMO) of the examined compounds (Z1–Z4).

4. Conclusions

A molecular docking study of sulfamidazole derivatives with the crystal structure of (PDB code 1KZN) enzyme revealed that these compounds interact with this enzyme satisfactorily. These results were reinforced by the low binding energy and high binding length with the active spots of the protein. The compounds Z2 and Z4 were found to have the highest docking score -6.2705 and -6.2108 , respectively. Moreover, the toxic, absorption, and physicochemical properties study of the prepared compounds aims to recognize the similarity of their features with drugs. It can be concluded that sulfamidazole derivatives could be utilized for drug improvement by designing and modifying compounds to be more active. Sulfamidazole derivatives compounds (Z1-Z4) were synthesized via a diazonium reaction and these compounds contain azo moiety. The compounds were characterized utilizing FT-IR, ^1H NMR, in addition to melting point measurements. Regarding study antibacterial study, against four bacterial strains (*E. coli*, *K. pneumonia*, *Salmonella*, and *S. aureus*). It was concluded that the azo compounds possess a moderate activity against all bacterial strains at ($100 \mu\text{g}/\text{ml}$) concentration. To sum up, the dye compounds (Z1-Z4) are very important and could be considered as an essential material for future active medications, especially when they are used as inhibitors for *E. coli*, *K. pneumonia*, *Salmonella*, and *S. aureus* bacteria.

Conflict of interest

The authors declare that they have no competing interests.

Acknowledgment

The authors are thankful to the University of Wasit and the College of Sciences, for providing us the facilities to achieve this work.

References

- [1] M.-Y. Zhao, Y.-F. Tang, G.-Z. Han, Recent advances in the synthesis of aromatic azo compounds, *Molecules* 28 (2023) 6741, <https://doi.org/10.3390/molecules28186741>.
- [2] R.A. Kamoon, M.M.J. Al-Mudhafar, T.N.-A. Omar, Synthesis, characterization and antimicrobial evaluation new azo compounds derived from sulfonamides and isatin schiff base, *Int J Drug Delivery Tech* 10 (2020) 150–155, <https://doi.org/10.25258/ijddt.10.1.22>.
- [3] I.H. Ibraheem, N.S. Mubder, M.A. Abdullah, H. Al-Neshmi, Synthesis, characterization and bioactivity Study from azo–ligand derived frommethyl-2-amino benzoate with some metal ions, *Baghdad Sci J* 20 (2023) 114–120, <https://doi.org/10.21123/bsj.2022.6584>.
- [4] S. Benkhaya, S. M'rabet, A. El-Harfi, Classifications, properties. recent synthesis and applications of azo dyes, *Heliyon* 6 (2020) e03271, <https://doi.org/10.1016/j.heliyon.2020.e03271>.
- [5] J.M. Barrera-Andrade, N.D.L. Fuente-Maldonado, R. Lopez-Medina, A.M. Maubert-Franco, E. Rojas-Garcia, Revolutionizing wastewater treatment: harnessing metal–organic frameworks for exceptional photocatalytic degradation of azo-type dyes, *Colorants* 2 (2023) 674–704, <https://doi.org/10.3390/colorants2040035>.
- [6] M. Mezher, M.A. Toma, A. Dala, H. Kaain, Synthesis and characterization of new azo dyes based on thiazole and assess the biological and laser efficacy for them and study their dyeing application, *Egypt J Chem* 64 (2021) 2903–2911, <https://doi.org/10.21608/ejchem.2021.55296.3163>.
- [7] K.M.A. Abdelmoteleb, M.A. El-Apasery, A.A.F. Wasfy, S.M. Ahmed, Synthesis of new monoazo disperse dyes for dyeing polyester fabric using two different dyeing methods: demonstration of their antibacterial and anticancer activities, *Polymers* 15 (2023) 3052, <https://doi.org/10.3390/polym15143052>.
- [8] M.D. Martino, L. Sessa, M.D. Matteo, B. Panunzi, S. Piotto, S. Concilio, Azobenzene as antimicrobial molecules, *Molecules* 27 (2022) 5643, <https://doi.org/10.3390/molecules27175643>.
- [9] F.F.S. Al-Abadi, Synthesis and characterization of azo dyes and study of the equilibrium and thermodynamics of adsorption of dyes on activated charcoal, *Mater Today Proc* 49 (2022) 2699, <https://doi.org/10.1016/j.matpr.2021.09.059>.
- [10] A.R. Sayed, H. Elsayy, S. Shaaban, S.M. Gomha, Y.S. Al-Faiyz, Design, synthesis, and biological evaluations of novel azothiazoles based on thioamide, *Curr Issues Mol Biol* 44 (2022) 2956–2966, <https://doi.org/10.3390/cimb44070204>.
- [11] A. Ragab, S.A. Fouad, O.A.A. Ali, E.M. Ahmed, A.M. Ali, A.A. Askar, Y.A. Ammar, Sulfaguanidine hybrid with some new pyridine-2-one derivatives: design, synthesis, and antimicrobial activity against multidrug-resistant bacteria as dual DNA gyrase and DHFR inhibitors, *Antibiotics* 10 (2021) 162, <https://doi.org/10.3390/antibiotics10020162>.
- [12] K. Pakeeraiah, S. Mal, M. Mahapatra, S.K. Mekap, P.K. Sahu, S.K. Paidsetty, Schematic-portfolio of potent anti-microbial scaffolds targeting DNA gyrase: unlocking ways to overcome resistance, *Int J Biol Macromol* 256 (2024) 128402, <https://doi.org/10.1016/j.ijbiomac.2023.128402>.
- [13] M. Durcik, T. Tomašič, N. Zidar, A. Zega, D. Kikelj, L.P. Mašič, J. Ilaš, ATP-competitive DNA gyrase and topoisomerase IV inhibitors as antibacterial agents, *Expert Opin Ther Pat* 29 (2019) 171–180, <https://doi.org/10.1080/13543776.2019.1575362>.
- [14] M. Castelli, G. Baggio, A.I. Ruberto, T. Rossi, A. Provvionato, M. Malagoli, R. Bossa, I. Galatulas, In vitro activity of trimethoprim in association with sulfimidazole against aerobic gram-negative and gram-positive microorganisms and Clostridia, *Chemotherapy* 141 (1995) 337–344, <https://doi.org/10.1159/000239365>.
- [15] D. Fernandez, A. Restrepo-Acevedo, C. Rocha-Roa, R.L. Lagadec, R. Abonia, S.A. Zacchino, J.A. Gómez Castaño, F. Cuenú-Cabezas, Synthesis, structural characterization, and in vitro and in silico antifungal evaluation of azo-azomethine pyrazoles(PhN₂(PhOH)CHN(C₃N₂ (CH₃)₃)PhR, R = H or NO₂), *Molecules* 26 (2021) 7435, <https://doi.org/10.3390/molecules26247435>.
- [16] J. Polak, M. Graż, K. Wlizio, K. Szalapatka, J. Kapral-Piotrowska, R. Paduch, A. Jarosz-Wilkotłazka, Bioactive properties of a novel antibacterial dye obtained from laccase-mediated oxidation of 8-Anilino-1-naphthalene sulfonic acid, *Molecules* 27 (2022) 487, <https://doi.org/10.3390/molecules27020487>.
- [17] N. Singh, V. Abrol, S. Parihar, S. Kumar, G. Khanum, J.M. Mir, A.A. Dar, S. Jaglan, M. Sillanpää, S. Al-Farraj, Synthesis, molecular docking, and in vitro antibacterial evaluation of benzotriazole-based β -amino alcohols and

- their corresponding 1,3-oxazolidines, *ACS Omega* 8 (2023) 41960–41968, <https://doi.org/10.1021/acsomega.3c07315>.
- [18] S. Martínez-Robles, E. González-Ballesteros, J. Reyes-Esparza, I. Trejo-Teniente, B.E. Jaramillo-Loranca, A. Téllez-Jurado, V.H. Vázquez-Valadez, E. Angeles, G.V. Hernández, Effect of β - hydroxy - γ - amino phosphonate (β - HPC) on the hydrolytic activity of *Nocardia brasiliensis* as determined by FT-IR spectrometry, *Front Microbiol* 14 (2023) 1089156, <https://doi.org/10.3389/fmicb.2023.1089156>.
- [19] S.A. Abouel-Enein, S.M. Emam, E.M. Abdel- Satar, Bivalent metal chelates with pentadentate azo-schiff base derived from nicotinic hydrazide: preparation, structural elucidation, and pharmacological activity, *Chem Biodivers* 20 (2023) e202201223, <https://doi.org/10.1002/cbdv.202201223>.
- [20] M. Ajaz, S. Shakeel, A. Rehman, Microbial use for azo dye degradation-a strategy for dye bioremediation, *Int Microbiol* 23 (2020) 149–159, <https://doi.org/10.1007/s10123-019-00103-2>.
- [21] A.F. Abdullah, S.H. Kathim, A.G. Sager, J.K. Abaies, Synthesis and identification of two dyes derived from p-amino phenol and study of their effectiveness as corrosion inhibitors: experimental and theoretical analysis, *Baghdad Sci J* 64 (March 2025) 1–14, in press.
- [22] J. Polak, K. Wlizio, R. Pogni, E. Petricci, M. Graz, K. Szalopata, M. Osińska-Jaroszuk, J. Kapral-Piotrowska, B. Pawlikowska-Pawlega, A. Jarosz-Wilkolazka, Structure and bioactive properties of novel textile dyes synthesised by fungal laccase, *Int J Mol Sci* 21 (2020) 2052, <https://doi.org/10.3390/ijms21062052>.
- [23] S.A. Alsaheb, Characterization and biological activity of some new derivatives derived from sulfamethoxazole compound, *Baghdad Science J* 17 (2020) 471–480, <https://doi.org/10.21123/bsj.2020.17.2.0471>.
- [24] E. Kellenberger, J. Rodrigo, P. Muller, D. Rognan, Comparative evaluation of eight docking tools for docking and virtual screening accuracy, *Proteins* 57 (2004) 225–242, <https://doi.org/10.1002/prot.20149>.
- [25] T.C. Ramalho, M.S. Caetano, E.F.F. da Cunha, T.C.S. Souza, M.V.J. Rocha, Construction and assessment of reaction models of class IEPSP synthase: molecular docking and density functional theoretical calculations, *Biomol Struct Dyn*. 27 (2009) 195–207, <https://doi.org/10.1080/07391102.2009.10507309>.
- [26] M.R. Kubba, K.F. Abood, DFT, PM3, AM1, and MINDO/3 quantum mechanical calculations for some INHCCs symmetry schiff bases as corrosion inhibitors for mild steel, *Iraqi J Sci* 56 (2015) 602–621. <https://ijs.uobaghdad.edu.iq/index.php/eijs/article/view/10278>.
- [27] A.G. Sager, J.K. Abais, Z.R. Katoof, Molecular docking, synthesis and evaluation for antioxidant and antibacterial activity of new oxazepane and benzoxazepine derivatives, *Baghdad Sci J* 11 (2023) 1–17, <https://doi.org/10.21123/bsj.2023.8553>.
- [28] H. Khelfaoui, D. Harkati, B.A. Saleh, Molecular docking, molecular dynamics simulations and reactivity, studies on approved drugs library targeting ACE2 and SARS-CoV-2 binding with ACE2, *J Biomol Struct Dyn* 39 (2021) 7246–7262, <https://doi.org/10.1080/07391102.2020.1803967>.
- [29] O. Michalak, M. Cybulski, W. Szymanowski, A. Gornowicz, M. Kubiszewski, K. Ostrowska, P. Krzeczyński, K. Bielawski, B. Trzaskowski, A. Bielawska, Synthesis, biological activity, ADME and molecular docking studies of novel ursolic acid derivatives as potent anticancer agents, *Int J Mol Sci* 24 (2023) 8875, <https://doi.org/10.3390/ijms24108875>.
- [30] P. Banerjee, A.O. Eckert, A.K. Schrey, R. Preissner, ProTox-II: a webserver for the prediction of toxicity of chemicals, *Nucleic Acids Res* 46 (2018) W257–W263, <https://doi.org/10.1093/nar/gky318>.
- [31] D. Gadaleta, K. Vuković, C. Toma, G.J. Lavado, A.L. Karmaus, K. Mansouri, N.C. Kleinstreuer, E. Benfenati, A. Roncaglioni, SAR and QSAR modeling of a large collection of LD50 rat acute oral toxicity data, *J Cheminf* 58 (2019) 1–16. <https://doi.1186/s13321-019-0383-2>.
- [32] L. Zhang, H. Zhang, H. Ai, H. Hu, S. Li, J. Zhao, H. Liu, Applications of machine learning methods in drug toxicity prediction, *Curr Top Med Chem* 18 (2018) 987–997, <https://doi.org/10.2174/1568026618666180727152557>.
- [33] V. Arjunan, S.T. Govindaraja, S.P. Jose, S. Mohan, DFT simulation, quantum chemical electronic structure, spectroscopic and structure-activity investigations of 2-benzothiazole acetonitrile, *Spectrochim Acta Mol Biomol Spectrosc* 128 (2014) 22–36.
- [34] A. Moreno-Ceballos, M.E. Castro, N. A Caballero, L. Mammino, F.J. Melendez, Implicit and explicit solvent effects on the global reactivity and the density topological parameters of the preferred conformers of caespitate, *Computation* 12 (2024) 1–21, <https://doi.org/10.3390/computation12010005>.
- [35] S.H. El-Demerdash, S.A. Halim, A.M. El-Nahas, A.B. El-Meligy, A density functional theory study of the molecular structure, reactivity, and spectroscopic properties of 2-(2-mercaptophenyl)-1-azaazulene tautomers and rotamers, *Sci Rep* 13 (2023) 15626, <https://doi.org/10.1038/s41598-023-42450-1>.
- [36] A.H. Bakheit, H.A. Abuelizz, R. Al-Salahi, Hirschfeld surface analysis and density functional theory calculations of 2-Benzyloxy-1,2,4-triazolo[1,5-a]quinazolin-5 (4H)-one: a comprehensive study on crystal structure, intermolecular interactions, and electronic properties, *Crystals* 13 (2023) 1410, <https://doi.org/10.3390/cryst13101410>.